INTERNATIONAL SCIENTIFIC JOURNAL
GEOGRAPHICA PANNONICA
Volume 27, Issue 3, 184–198 (September 2023)
Contents lists available at ScienceDirect
Journal homepage: http://www.dgt.uns.ac.rs/en/homepage/pannonica/

Extreme Precipitations and their Influence on the River Flood Hazards – A Case Study of the Sana River Basin in Bosnia and Herzegovina

Luka Sabljić[A*], Dragoslav Pavić[B], Stevan Savić[B], Davorin Bajić[A]

[A] *University of Banja Luka, Faculty of Natural Sciences and Mathematics, Mladena Stojanovića 2, 78000 Banja Luka, Bosnia and Herzegovina, luka.sabljic@pmf.unibl.org; davorin.bajic@pmf.unibl.org*

[B] *University of Novi Sad, Faculty of Sciences, Department of Geography, Tourism and Hotel Management, Trg Dositeja Obradovića 3, 21000 Novi Sad, Serbia, dragoslav.pavic@dgt.uns.ac.rs; stevan.savic@dgt.uns.ac.rs*

KEYWORDS

climate change
precipitation
water level
flood
remote sensing
mapping
risk zones

ABSTRACT

The subject of the research paper is the use of remote sensing in monitoring and analyzing the impact of climate change on the occurrence of extreme precipitation, and the cause-and-effect occurrence of floods in the area of the Sana River Basin in Bosnia and Herzegovina. The goal is to process the "product" of remote sensing to identify the time intervals of occurrence of extreme precipitation, to assess their impact on water levels, and to map potential floods in space. Spatial identification of zones that are at risk of flooding is an integral part of the aforementioned goal. Precipitation monitoring was performed by processing Climate Hazards Group InfraRed Precipitation with Station Data through the Google Earth Engine platform. The observed 30-year period (1992–2022) was compared with the average precipitation for 2017, 2018 and 2019. The impact of extreme precipitation on the water level of the Sana River was analyzed. Flooding periods have been identified: February and December 2017, March 2018 and May 2019. Mapping of flooded areas was carried out by pre-processing and post-processing of Sentinel-1 radar satellite images. The total flooded area is: 710.38 ha (February 2017), 496.79 ha (December 2017), 417.86 ha (March 2018) and 422.42 ha (May 2019). Based on the identified flooded areas, a flood risk map was created on the main course of the Sana River. The research contributes to a better understanding of the changes that occur in the area under the influence of climate change, and the data presented are important for numerous practical issues in the field of water resource management and flood protection.

Introduction

Climate change poses a threat to people around the world (IPCC, 2021). Changes in the intensity and frequency of climate change lead to the occurrence of extreme events, such as heavy and intense precipitation, which have a major impact on the management of water resources and flood risks (Meresa et al., 2022). Extreme precipitation affects the intensity and frequency of floods, creating major problems for aquatic and terrestrial ecosystems, including human societies and economies (Tabari, 2020). The monitoring of heavy precipitation intensity and frequency ena-

* Corresponding author: Luka Sabljić, luka.sabljic@pmf.unibl.org

doi: 10.5937/gp27-45600

Received: July 20, 2023 | Revised: August 19, 2023 | Accepted: September 08, 2023

bles the tracking of climate change effects (Bucchignani et al., 2016; Dong et al., 2021).

Today, it is possible to monitor precipitation based on the comparison of data from several sources. Data from hydrological and meteorological stations, and satellite data can be considered (Michaelides et al., 2009; Bai et al., 2018). Precipitation data obtained from hydrological and meteorological stations have high accuracy (Kidd et al., 2017), but they are spatially limited (Brocca et al., 2019). On the other hand, data obtained from weather radars have limiting characteristics in terms of data quality due to signal distortion (Raghavan, 2013). Satellite precipitation data cover large regions with high spatial and temporal resolution. The mentioned type of data has its shortcomings, which can be reduced to a minimum by post-processing actions (Maggioni et al., 2016). Accordingly, it is necessary to validate the satellite data on the estimation of precipitation based on the data of meteorological stations, to assess their precision and possibility of use (Loew et al., 2017; Kumar et al., 2019).

Extreme precipitation can lead to floods, which can result in big economic and human losses (Ward et al., 2013). For this reason, flood mapping and modelling processes are very important, in order to adequately assess the flood risk (Moel et al., 2009), but also the damage caused by this primary hydrological hazard (Amadio et al., 2016). Remote sensing "products" in the form of satellite images play a very important role in flood mapping and modelling, as well as modern platforms whose purpose is the efficient processing of this data. One such platform for geospatial processing of satellite data is Google Earth Engine (GEE). The mentioned platform is based on the cloud technology, and with it, it is possible to easily overcome the challenges and problems faced by traditional approaches when processing satellite images (Gorelick et al., 2017). There is a significant number of research whose focus is the analysis of climate change based on the processing of satellite images using the GEE platform (Pandey et al., 2022; Nghia et al., 2022; Rincón-Avalos et al., 2022).

The main objective of the present research paper is to monitor the impact of climate change on the occurrence of primary hydrological hazard in the form of floods. An integral part of the aforementioned goal is the identification of extreme precipitation that leads to flooding, and the identification of areas that are at risk of flooding. The research is based on the use of modern technologies, such as geographic information systems (GIS) and remote sensing. Therefore, the general novelty and importance of this study are answering the following scientific questions (SQ): SQ1 – To better understand the impact of climate change on the occurrence of extreme precipitation and the cause-and-effect occurrence of floods; SQ2 – To present the methodology that could be important for the identification of flooded areas after a natural disaster, and can be useful for many practical issues, such as the timely action of the competent institutions in order to prevent a large-scale disaster, assessing the consequences and identifying critical points for the construction of embankments and other protecting systems for preventing floods in the future.

Study area

The research area is the Sana River basin (SRB) located in Bosnia and Herzegovina (B&H) (Figure 1). The main geographical characteristics of the research area are given in Table 1. As part of the research, the emphasis was placed on the main course of the Sana River. The aforementioned river originates in Donja Pecka and is the largest tributary of the Una River. The source is located at 414 m above sea level, and the confluence is at 122 m above sea level. The main course of the Sana River is 146 km long. It is characterized by the Posavina variant of the pluvial-naval water regime, characterized by the highest water level in April and the lowest in August (Gnjato, 2018). According to the Köppen-Geiger climate classification (Kottek et al., 2016), the research area belongs to the Cfb climate type, which is characterized by moderately cold winters and warm summers.

Table 1. The main geographical characteristics of the SRB

Type of SRB geographical characteristic	SRB geographical information
Spatial distribution by municipalities	Novi Grad, Kostajnica, Prijedor, Oštra Luka, Bosanska Krupa, Banja Luka, Sanski Most, Ključ, Ribnik, Mrkonjić Grad, Krupa na Uni
Latitude	44.18°N–45.09°N
Longitude	16.29°E–17.09°E
Total geographic area (km²)	about 3470 km²
Average altitude	505 m
Average slopes	10.9°
Population number (in the thousands)	454
Spatial share in Sava basin (in %)	3.55

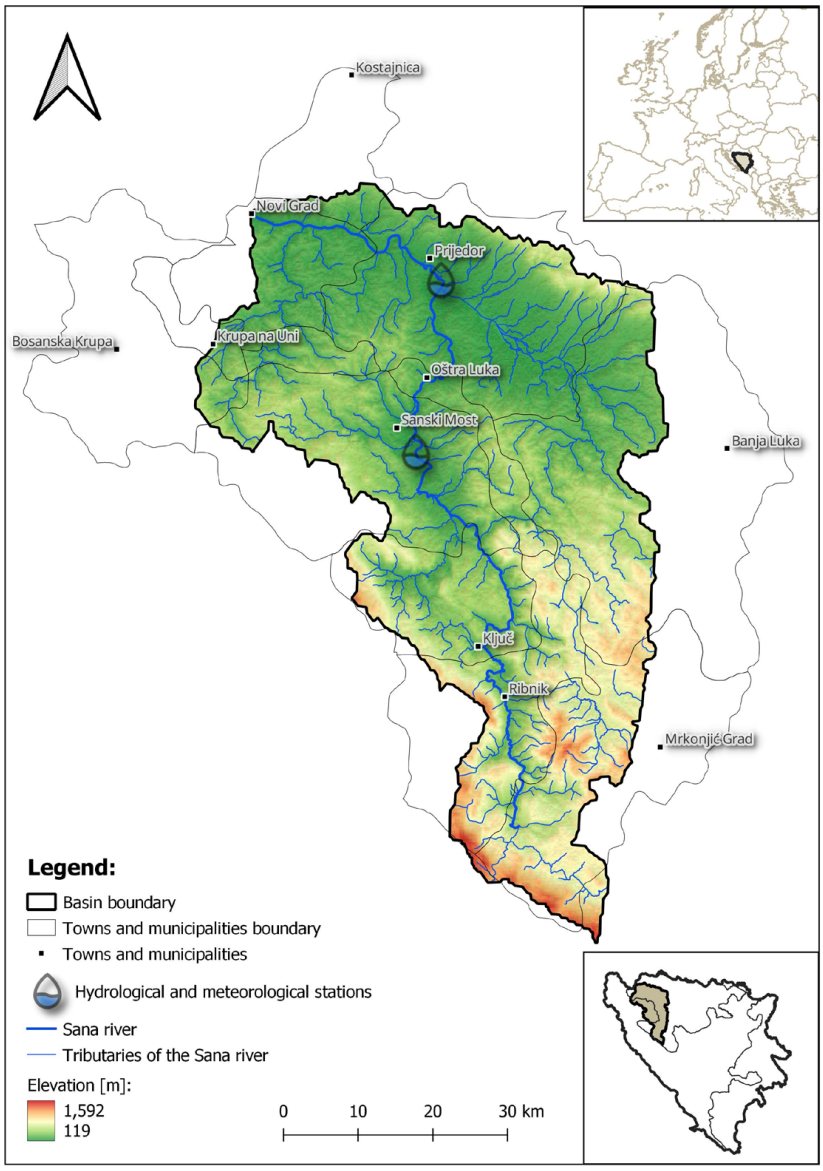

Figure 1. Location of the study area

Data used

Several input data were used in the research. The boundary of the SRB was taken from the HydroSHEDS database (https://www.hydrosheds.org/). The river network within the basin was taken from the EU-Hydro River Network Database (https://land.copernicus.eu/). Input data on precipitation were collected from meteorological stations Prijedor (44.97° N–16.70° E) and Sanski Most (44.77° N–16.67° E), while data on water level were collected from hydrological (HS) stations of the same name and location. The mentioned stations are not the only ones in the study area, but they are the only ones with complete, continuous and publicly available data for the defined time period of the research. The basis of the research is represented by satellite data on precipitation estimation called Climate Hazards Group InfraRed precipitation with Station data (CHIRPS). Mapping of flooded areas was performed by pre-processing and post-processing of radar Sentinel-1 satellite images.

Since 2014 the University of California, Santa Barbara distributes CHIRPS precipitation estimation data at different time intervals (daily, 5-day, 10-day, and monthly) (Funk et al., 2015). The precipitation data set is of a global character, and has relatively high spatial resolution data (0.05° x 0.05° ~ 5.3 km) and a long-term time coverage (1981 – almost real-time). The CHIRPS data processing algorithm combines satellite and measured precipitation estimates. All over the world, this type of data is subjected to the method of comparison with data obtained from meteorological stations. According to research, in terms of

bias and Pearson correlation coefficient, the CHIRPS dataset performs relatively well at the regional and global scale compared to other modern satellite precipitation data (Beck et al., 2017; Bai et al., 2018; Dinku et al., 2018).

Sentinel-1 are radar satellite images with high spatial resolution (10 m) and relatively good temporal resolution (about 6 days). The specification of these radar satellite images includes high-resolution Ground Range Detected, SAR sensor with C band (5.405 GHz), Interferometric Wide swath, from 30.4° to 46.2°, wide bandwidth (250 km) and double polarization (VV and VH) (Tran et al., 2022; Plank et al., 2014).

Methods

The process of monitoring the impact of climate change on precipitation, as well as the process of mapping flooded areas, was carried out by processing satellite data. The GEE platform based on cloud technology was used for processing. The research includes the processing and use of satellite data on precipitation, deviations in precipitation patterns, identification of extreme precipitation, assessment of the consequences on the water level, cause-and-effect mapping of flooded areas, and identification of spatial zones that are at risk of flooding. The research time period for precipitation is 1992–2022 year, and for the water level 2001–2019 year. The identification of flooded areas was carried out for the reference years (2017, 2018 and 2019).

The process of validating satellite data on precipitation was performed by comparing the mentioned data with data obtained from meteorological stations. The data on the average amount of precipitation per month for the defined time period of the research were validated. In order to find the interdependence between the impacts of climate change on precipitation, the 30-year average precipitation (1992–2022) was compared with the reference years (2017, 2018 and 2019). The goal is to identify precipitation extremes during reference years that "bounce" from the 30-year average precipitation. In parallel with this process, data on the average water level were also considered, in order to establish the reflection of extreme precipitation on the water level. Data on the average mean water level for the research period (2001–2019) were compared with the data of the reference years (2017, 2018 and 2019) (Figure 2). The goal of the presented approach is the spatial identification of the flood, which due to the extreme water level should occur first at the HS location, and then causally and consequently at other locations in the basin. The periods in which there is a clear difference in the amount of

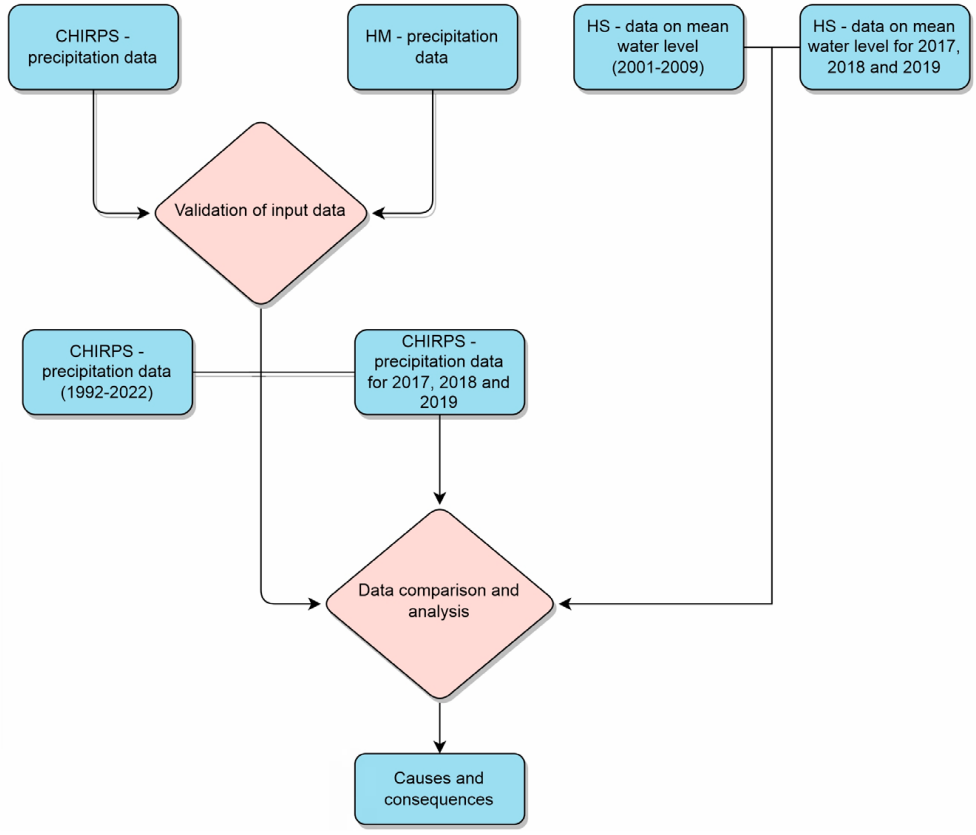

Figure 2. Algorithm for processing data on precipitation and water levels

precipitation, and a clearly differentiated extreme level of water, represent temporal data for the mapping procedure and determining the spatial extent of flooding in the research area.

The process of mapping flooded areas was carried out by pre-processing and post-processing of Sentinel-1 radar satellite images (Figure 3). The first step represents the filtering of satellite image characteristics (product type, polarization and sensor operation mode). Automated pre-processing of the filtered satellite image is then performed (reducing the image to the study area, applying orbit file and thermal noise removal). A post-processing process was performed on the pre-processed satellite images. For selected time periods within the reference years (before and during/after floods), two mosaics are created in the form of raster data models – the first mosaic to map the permanent part of the watercourse, and the second to map the spatial extent of the flooded areas. A speckle filtering procedure is applied to both mosaics, in order to reduce the possibility of incorrectly mapping areas that do

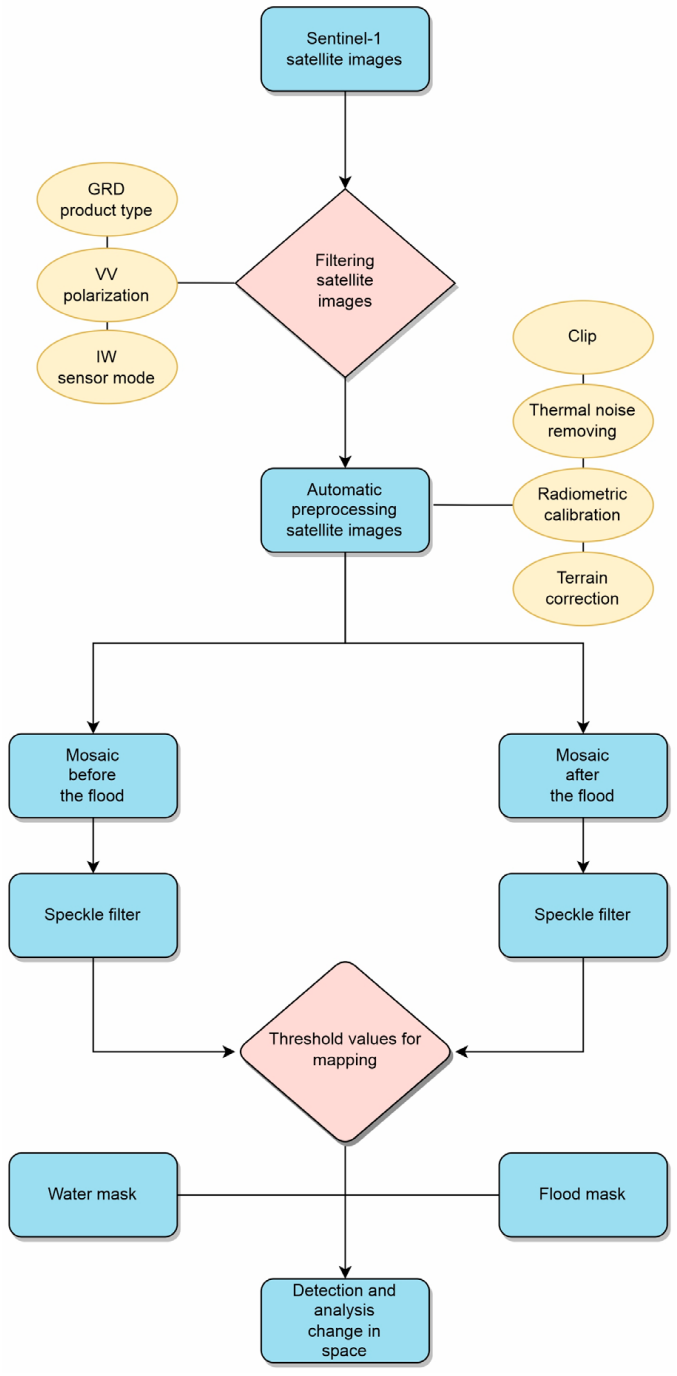

Figure 3. Algorithm for processing satellite images for flood mapping

not represent water bodies as water bodies. A filtered mosaic in the form of a raster data model is the basis for mapping. The mapping process is carried out on the basis of the numerical value of pixels, that is, through the definition of a numerical threshold value for distinguishing flooded areas from other areas. With this process, the final result is obtained in the form of a permanent water surface mask and a flooded surface mask, over which the process of detecting and analyzing changes in space is performed, as well as the process of identifying zones at risk of flooding.

Results

The validity assessment of CHIRPS satellite data on precipitation estimation was performed by comparing the same with data obtained from meteorological stations Prijedor and Sanski Most for a 30-year time period (1992–2022). CHIRPS satellite data on spatial precipitation estimates vary, where each pixel depicts a different precipitation value for the area it covers. As part of this research, in order to evaluate the validity of CHIRPS data, algorithms were developed using the GEE platform. The CHIRPS average amount of precipitation per month at the level of the entire research area was calculated (one numerical value in the form of the average amount of precipitation for each month of the year for a 30-year time period). On the other hand, taking into account orography of the area (in accordance with the location of the stations), data from meteorological stations Prijedor and Sanski Most were combined. Based on the combined data of both meteorological stations, the average amount of precipitation per month for the mentioned 30-year time period was calculated. The obtained results were compared with each other (Figure 4). During April and September, the CHIRPS data almost matches the meteorological data. January, February, March, May, June, July, August and October are characterized by minimal deviation of CHIRPS data from real ones (< 8%). A significant deviation is visible during November and December. The reason for the deviation in the mentioned months is explained by the occurrence of snowfall, which caused a partial distortion of the satellite data. Likewise, the challenge of comparing "polygon" and "point" data needs to be considered. Namely, the CHIRPS data depict the average value of the amount of precipitation per month in the entire basin area, while the data on the average amount of precipitation from meteorological stations refer to two locations in the area of the basin. In this respect, it is necessary to point out the lack of a meteorological station at higher altitudes of the basin. In addition to the meteorological stations Prijedor and Sanski Most, there are no other stations at the level of the study area that have continuous data for the defined time period of the research. Considered all the above mentioned, as well as the presented comparison results, it is concluded that the CHIRPS data are valid for the further research.

CHIRPS monthly average precipitation data (1992–2022) are overlaid with monthly average precipitation for reference years (Figure 5). The goal for reference years is to identify months with a significantly higher amount of precipitation then the 30-year average. According to the authors, months with a higher amount of precipitation represent those where the average amount of precipitation is > 20 mm in relation to the average amount of precipitation per month during the 30-year period. During 2017, a higher amount of precipitation than the 30-year average was

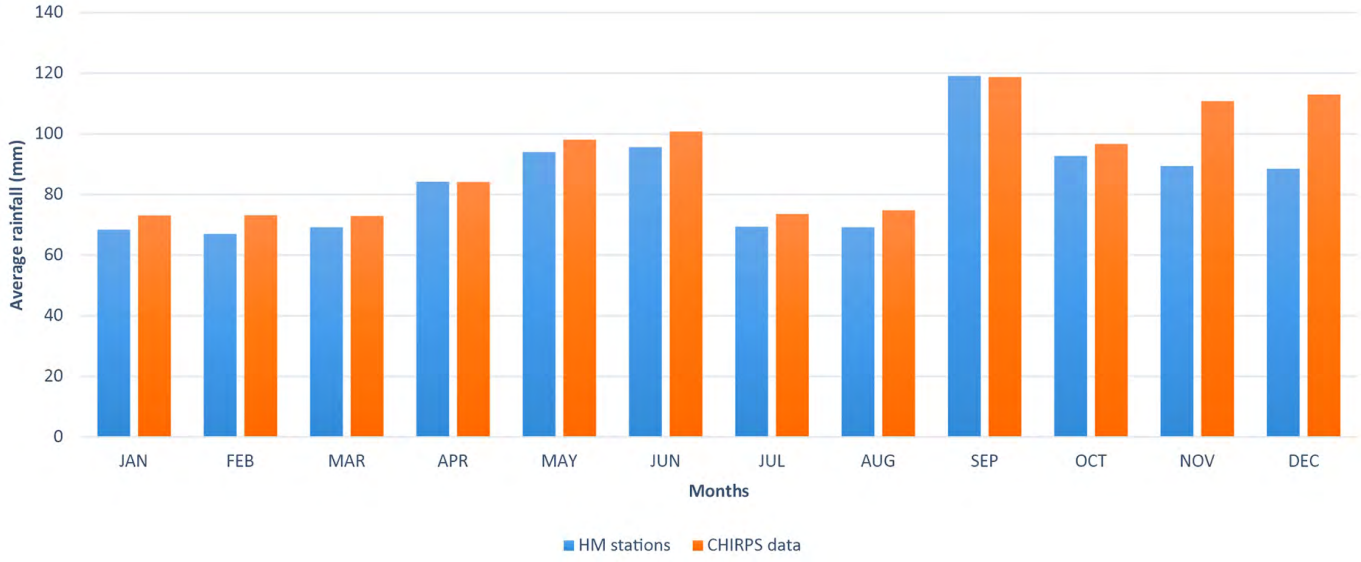

Figure 4. Average precipitation by month (1992–2022) for study area

Figure 5. Comparison of the CHIRPS average amount of precipitation by month (1992–2022; 2017, 2018 and 2019)

recorded in February (> 21.2 mm), September (> 61.6 mm) and December (> 57.2 mm). A higher amount of precipitation during 2018 is visible in February (> 40.1 mm), March (> 79.1 mm), May (46.2 mm) and June (> 28.7 mm). During 2019, a higher amount of precipitation was recorded in May (> 69.5 mm), November (> 45.6 mm) and December (> 42.4 mm). Indicatively, there is a well-founded suspicion that during the months with a higher amount of precipitation than the 30-year average, floods could have occurred at the level of the study area.

In order to more clearly differentiate the time periods of occurrence of floods in the study area, the impact of recorded extreme precipitation on the water level of the Sana River was analyzed. For this reason, the data on the average mean water level by month (2001–2019) are overlaid with the average mean water level during the reference years (2017, 2018 and 2019) (Figure 6). The goal for the reference years is to identify the months whose average mean water level is higher than the 18-year average. According to the authors, the months during which the average mean water level is > 25 cm compared to the 18-year average can be interpreted as the time period when the floods occurred, and when it can be clearly mapped in space by processing satellite images. It is possible to identify floods in space even during smaller increases in the mean water level, but due to limitations in terms of the spatial resolution of satellite images, it is not possible to map them accurate and precise. The extreme amount of precipitation from February 2017 were reflected in the average mean water level of HS Prijedor (115 – 155 cm), and the same trend continued during the month of March (154.6 – 173 cm). During February 2017, a small difference in the increase of the average mean water level was noticeable on HS Sanski Most (172.2 – 176 cm). The extreme amount of precipitation in September of the mentioned year did not affect the average water level. The occurrence of extreme precipitation that did not affect the water level can be explained by the fact that during the previous months (May–August) the amount of precipitation was less than the 30-year average. During the mentioned period, the ground was not saturated with water, and therefore the precipitation that occurred during this period could not cause a higher water level, nor the potentional occurrence of floods. Extreme amounts of precipitation in December 2017 were reflected in the average mean water level of HS Prijedor (105.4 – 133 cm) and HS Sanski Most (169.3 – 178 cm). The trend from December 2017 continued in January 2018, so during the mentioned period a higher level of the average mean water level was recorded at HS Prijedor (99.5 – 144 cm) and HS Sanski Most (166.1 – 169 cm). The precipitation in February did not significantly affect the average water level, which for this month was almost identical to the 30-year average at HS Prijedor, while at HS Sanski Most it was below the 30-year average. The extreme amount of precipitation from March 2018 was reflected in the average mean water level of HS Prijedor (154.6 – 256 cm) and HS Sanski Most (196.5 – 239 cm). In addition to extreme precipitation, the melting of snow in the higher altitudes of the basin could potentially have contributed to the water level for March 2018. The trend of higher precipitation in May and June 2018 was not followed by a noticeably high average water level. Precipitation from May 2019 had a significant effect on the average mean water level of HS Prijedor (101.3 – 183 cm) and HS Sanski Most (172.4 – 186 cm). Due to the lower amount of precipitation in October, the precipitation from November did not leave a clearly visible mark on the average mean water level, while for the month of December the differences are negligible.

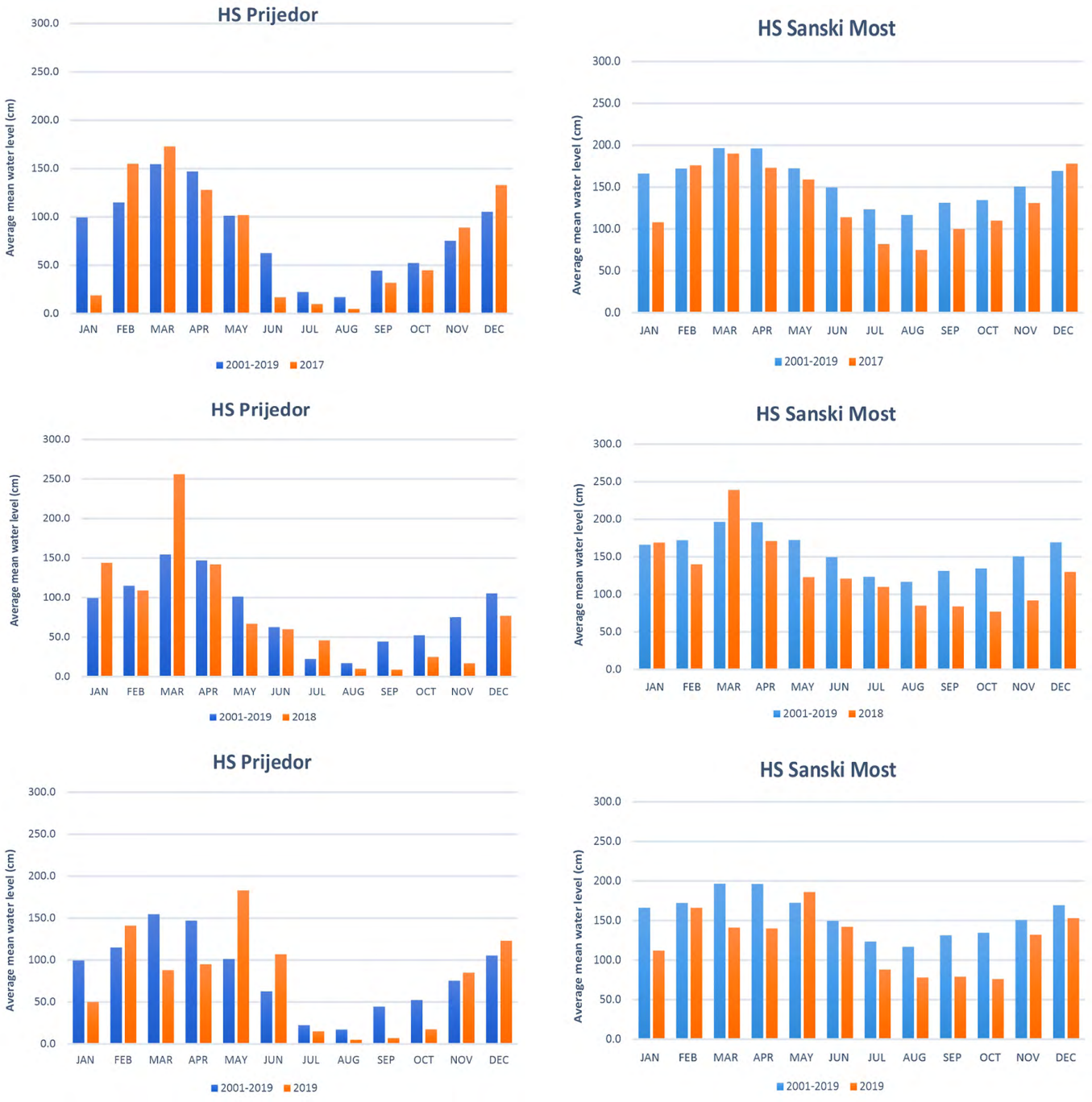

Figure 6. Comparison of the average mean water level of HS Prijedor and HS Sanski Most (2001–2019; 2017, 2018 and 2019)

Based on the comparative analysis of the average amount of precipitation during the 30-year period and the reference years, and the comparative analysis of the average mean water level for the 18-year period and the reference years, it is concluded that the potential mapping of floods with clearly separated spatial extents can be determined for February and December (2017), March (2018) and May (2019).

By applying the remote sensing method, and by processing and analyzing radar Sentinel-1 satellite images, flood mapping algorithms were developed. Running the algorithms through the GEE platform, the mapping of flooded areas was carried out at the level of the study area for previously defined time periods (Figure 7). The mapped flooded areas from February and December 2017, as well as March 2018, have similar spatial extents. During the mentioned periods of time, there was a dominant overflow of the river Sana from the riverbed in its middle and lower course. Also, during all three mentioned periods, there was a significant overflow of the Japra River, which is a left tributary of the Sana River. The total flooded area of the floods from February (2017) is 409.44 ha, December

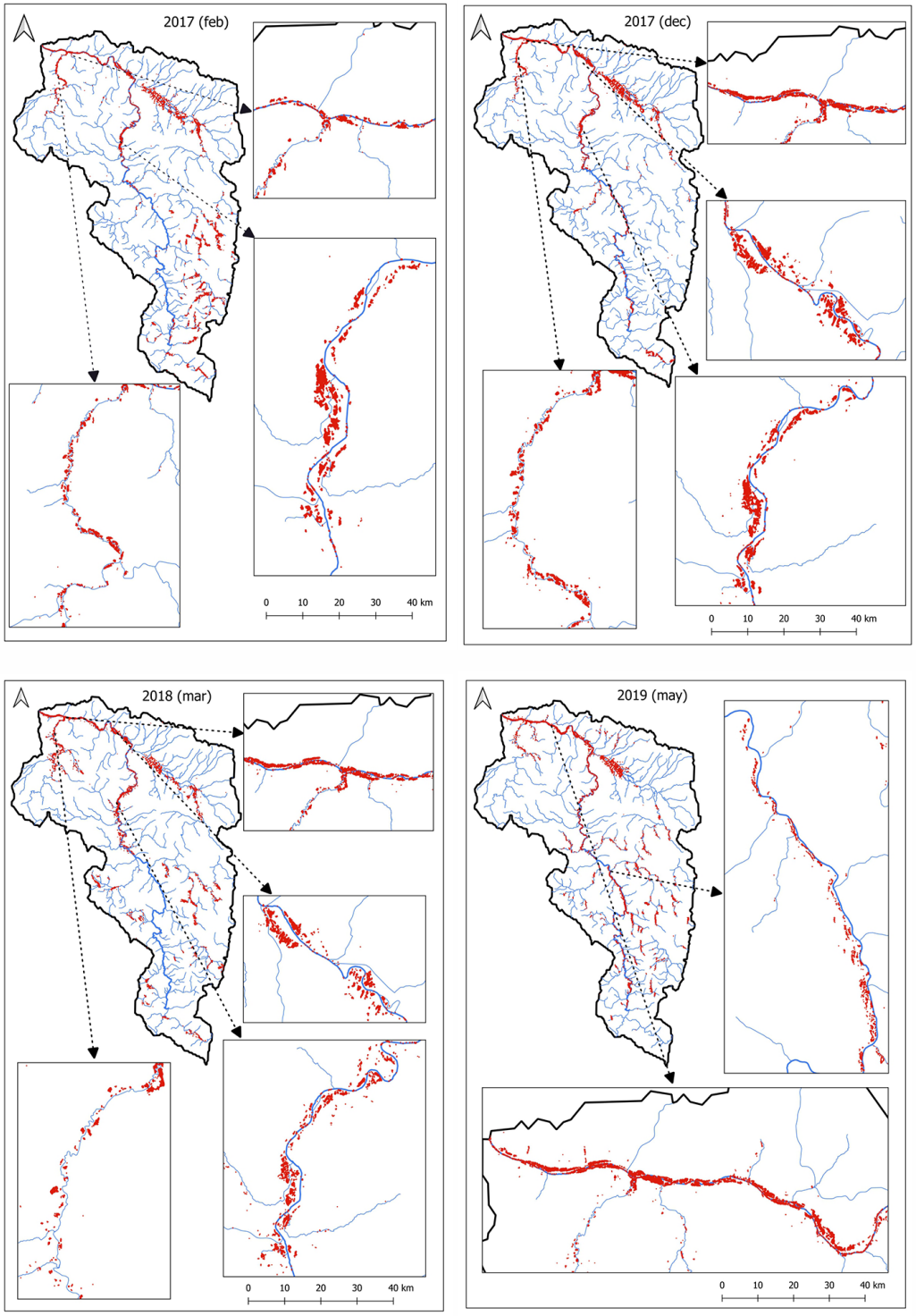

Figure 7. Mapped flooded areas

(2017) 497.10 ha and March (2018) 417.88 ha. The floods of May 2019 were characterized by the dominant overflow of the Sana River in the lower reaches in the area of the municipality of Novi Grad and the city of Prijedor, while the overflow and flooding of the Japra were insignificant. The total flooded area in May 2019 was 422.54 ha. Given that the mapped floods are characterized by a similar spatial extent, it is concluded that the municipalities and cities that were most affected by the floods were: Novi Grad, Prijedor, Oštra Luka, Sanski Most and Ključ.

The map of flooded areas from 2017, 2018 and 2019 was the basic input data for creating a map of flood risk zones, and it was created for the main course of the Sana River, i. e. the cities and municipalities that were most affected

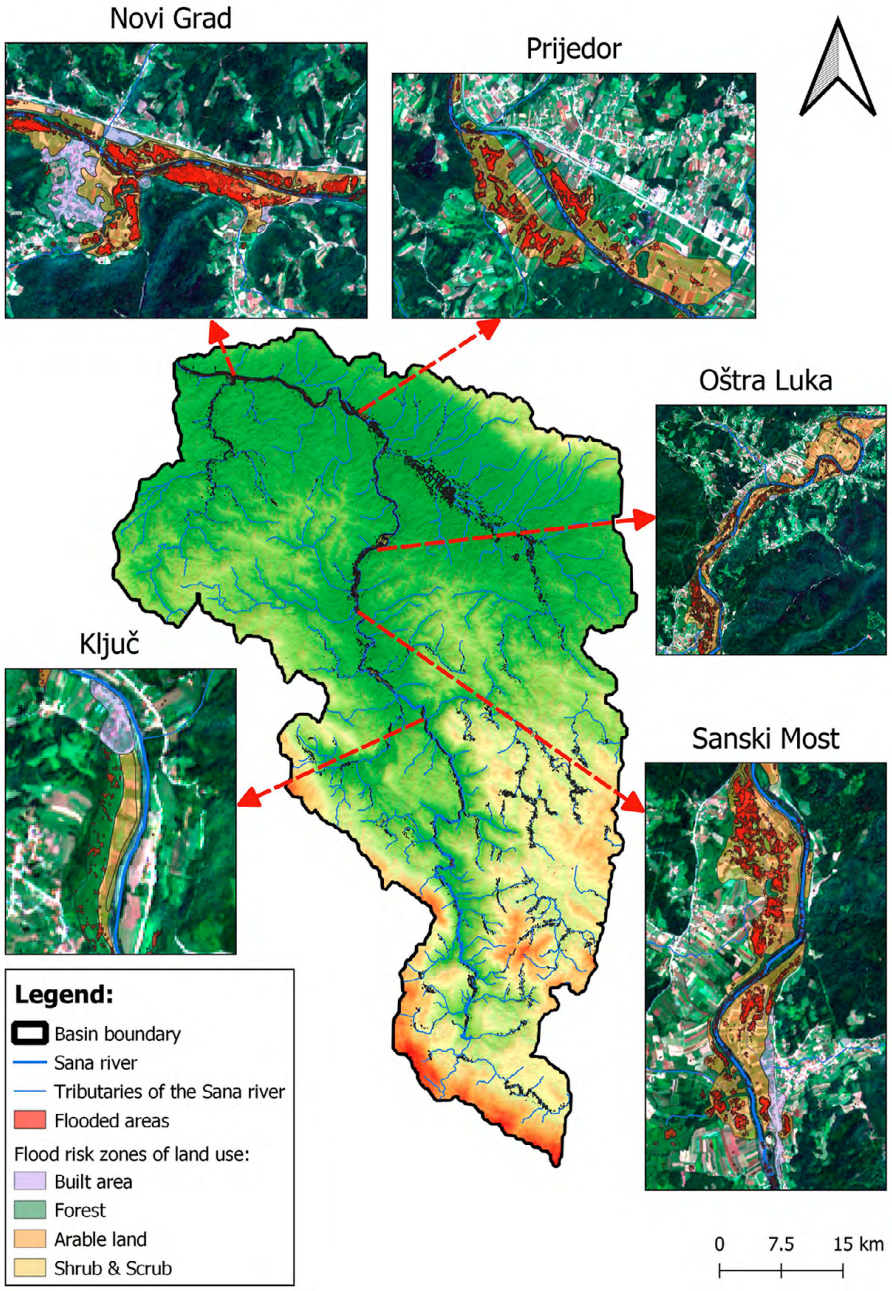

Figure 8. Flood risk zones

by floods (Novi Grad, Prijedor, Oštra Luka, Sanski Most and Ključ) (Figure 8). Based on the successive overlapping of mapped floods from the mentioned years and the satellite base, the ways of land use located in the flood risk zones were identified, which include: built areas, forest areas, arable land and scrub & shrub.

In Novi Grad, the total area of the floods risk zone is 666.63 ha, of which 71.97 ha are built areas, 62.38 ha of forest areas, 488.33 ha of arable areas and 43.95 ha of shrub & scrub areas. Bulit areas that are at risk of flooding include the urban center of the municipality and settlements: Blagaj Japra, Svodna, Blagaj Rijeka, Vitasavci and Trgovište. According to the last census from 2013, 11,923 inhabitants live in the threatened area (Republika Srpska Institute of Statistics, 2017). The total area of the flood risk zone in the city of Prijedor is 616.59 ha, of which 48.88 ha are built areas, 50.46 ha are forest areas, 500.23 ha are arable areas and 17.02 ha are shrub & scrub areas. Built areas that are at risk of flooding include the urban center of the city and settlements: Rasavci, Brezičani, Čarkovo, Ništavci, Gomjenica, Miljakovci and Donja Dragotina. According to the last census from 2013, 34,636 inhabitants live in the threatened area (Republika Srpska Institute of Statistics, 2017). The municipality of Oštra Luka is smaller in area than Novi Grad and Prijedor, so its total area of the flood risk zone (260.79 ha) is therefore smaller. The area of

land use that is at risk of flooding in Oštra Luka is 8.47 ha for built areas, 15.74 ha for forest areas, 225.32 ha for arable areas and 11.26 ha for shrub & scrub areas. Built areas that are at risk of flooding include the urban center of municipality and settlements: Koprivna and Usorci. According to the last census from 2013, the total number of inhabitants who live in the threatened area is 1,725 (Republika Srpska Institute of Statistics, 2017). In Sanski Most, a total of 408.64 ha are at risk of flooding, of which 15.42 ha are built areas, 40.93 ha are forest areas, 339.67 ha are arable areas and 12.62 ha are shrub & scrub areas. Built areas that are at risk of flooding include the urban center of municipality and settlements: Trnova, Vrhpolje and Sasina. According to the last census from 2013, 20,025 inhabitants live in the threatened area (Agency for Statistics of Bosnia and Herzegovina, 2019). Ključ is the municipality with the smallest area of risk of flooding compared to the other analyzed municipalities and cities. The total area of the flood risk zone is 108.39 ha, of which 6.68 ha are built areas, 73.77 ha are forest areas, 26.16 ha are arable areas and 1.78 are shrub & scrub areas. Built areas that are at risk of flooding include the urban center of municipality and settlement Kamičak. According to the last census from 2013, the total number of inhabitants who live in the threatened area is 5,800 (Agency of Statistics of Bosnia and Herzegovina, 2019) (Table 2).

Table 2. Types of land use under the risk of flooding

	Built areas (ha)	Forest (ha)	Arable land (ha)	Shrub & Scrub (ha)	Total (ha)
Novi Grad	71.97	62.38	488.33	43.95	666.63
Prijedor	48.88	50.46	500.23	17.02	616.59
Oštra Luka	8.47	15.74	225.32	11.26	260.79
Sanski Most	15.42	40.93	339.67	12.62	408.64
Ključ	6.68	73.77	26.16	1.78	108.39
Total (ha)	151.42	243.28	1579.81	86.63	2061.04

A total of 151.42 ha of built area, 243.28 ha of forest area, 1579.81 ha of arable area and 86.63 ha of shrub & scrub areas are under the flood risk zone in the observed area. The total area at risk of flooding is 2061.04 ha, of which 666.63 in Novi Grad, 616.59 ha in Prijedor, 260.79 ha in Oštra Luka, 408.64 ha in Sanski Most and 108.39 ha in Ključ. The total number of inhabitants of populated areas within which the zones of risk of flooding of built areas have been identified amounts to 74,109. Identified spatial areas located in the flood risk zone should in the future represent priority areas for the construction of systems and infrastructure in the function of flood protection.

Discussion

During the last decade, an increased frequency of years with extreme precipitation that resulted in catastrophic floods has been observed in B&H (Popov et al., 2017). Within this research, the occurrence of extreme precipitation in the area of the SRB is based on the processing of CHIRPS satellite data on precipitation estimation. According to Pacca et al. (2020), CHIRPS are characterized by homogeneous, standardized and continuous time series of data. The research results of the mentioned authors point out that CHIRPS data are significant for areas characterized by a small number of meteorological stations. Given that there are only two meteorological stations with continuous data for a 30-year time period (1992–2022) in the area of SRB, CHIRPS data represent the optimal solution for monitoring and identifying extreme precipitation. Ciric et al. (2018) successfully ranked precipitation extremes according to duration (1, 3, 5, 7 and 10 days) for the Danube River Basin area based on CHIRPS data. Gao et al. (2018) investigated the long-term characteristics of precipitation in the Xinjiang region of China (1983–2014). According to the results of the mentioned authors, CHIRPS performs well with respect to monthly and annual precipitation data. Zhang et al. (2022) conclude that CHIRPS data show high accuracy in precipitation estimation (coefficient of determination $R^2 < 0.92$). Bai et al. (2018) compared CHIRPS data with precipitation data from meteorological stations in China (1981–2014). The results showed a good agreement of CHIRPS (compared to data from meteorological stations) in areas characterized by a higher amount of precipitation. However, according to Paredes-Trejo et al. (2020) CHIRPS has limitations in reproducing the orographic precipitation due to the adoption of a fixed IRP CCD threshold value (i.e., 235 K), leading to classify warm orographic clouds as nonprecipitating (Dinku et al., 2018). Even though orographic clouds are relatively warm, they can produce substantial amounts of rain (Correia Filho et al., 2019). Wu et al. (2019) conclude that CHIRPS data perform well in estimating average monthly precipita-

tion, but also overestimate total annual precipitation. In the area of the SRB, a high degree of agreement between CHIRPS data and data from meteorological stations were established. However, looking at the months, a minimal overestimation of the CHIRPS data in relation to the data from meteorological stations is noticeable, and the same result is also visible on the summary average of precipitation for the 30-year period (1006.7 mm [meteorological data] – 1089.71 mm [CHIRPS]). Katsanos et al. (2016) established for the Cyprus area (1981–2010) a high degree of correlation of CHIRPS data regarding the identification of extreme precipitation. The mentioned authors emphasize the high correlation of CHIRPS extreme precipitation in relation to meteorological precipitation data in January, February and December. Their results indicate that meteorological stations at higher altitudes have a higher degree of correlation with CHIRPS data. A similar matching pattern is also visible in the SRB, where January, February and March are characterized by matching CHIRPS data by > 92% compared to meteorological data. The smaller data match in December is explained by the lack of meteorological station at higher elevations of the basin, which, taking into account the results of the aforementioned research, would affect the overall greater matching of precipitation throughout the year, and especially during the winter months.

As part of this research, thanks to CHIRPS data, the occurrence of extreme precipitation was observed three years in a row (2017, 2018 and 2019). In addition to extreme precipitation, in the area of the SRB, Ivanišević et al. (2022) established the number of days with higher water levels (2018 and 2019) that exceeded the emergency flood protection elevation. The presented results indicate the regularity of the occurrence of extreme precipitation, which leads to higher water levels, and the cause-and-effect occurrence of floods. The aforementioned results and research are supported by the successful mapping of flooded areas along the Sana River in 2019 (Sabljić & Bajić, 2021). According to Prokić et al. (2019) flooding is the most widespread natural hazard in Europe. Modern technologies and data, such as GIS and remote sensing, play a very important role in monitoring and identifying flooded areas. DeVries et al. (2020) developed algorithms for efficient flood mapping in the area of Texas (USA), Greece and Madagascar by processing Sentinel-1 and Landsat satellite images using GEE platform. Vanama et al. (2020) successfully mapped floods caused by extreme precipitation in August 2018 in India. The results of the mentioned authors in the form of mapped floods based on the processing of Sentinel-1 radar satellite images are based on the application of a numerical threshold value, and according to similar principle, by processing the same satellite images, floods were successfully mapped in the area of SRB. In addition to the mapping of the flooded areas, it is necessary to look at the consequences that the flood has on the environment. According to the results of Sarkadi et al. (2022) on the basis of satellite and other spatial data, flood susceptibility maps on the territory of Hungary were created. Samuele et al. (2021) mapped the floods in the area of northwestern Italy that were caused by the overflowing of the Sessia River. The result of research by the aforementioned authors determined that agricultural areas were the most affected by floods. Similar to the mentioned results, on the basis of the mapped flooded areas in the SRB, a map of the risk of flooding of various uses was created, which established the vulnerability of agricultural areas in the first place.

Conclusion

Monitoring of climate changes at the level of the study area for a defined period of time identified extreme precipitation, which was reflected in the water level, and causally and consequently caused the appearance of a primary hydrological hazard in the form of flooding. The identification of extreme precipitation three years in a row with catastrophic consequences in the form of floods indicates the negative impact of climate change in the research area. Thanks to advanced technologies such as GIS and remote sensing, as well as pre-processing and post-processing capabilities of satellite data, recurring patterns of floods with similar spatial characteristics during 2017, 2018 and 2019 have been identified. It was established that the municipalities through which the Sana River flows are the most affected by floods in the basin area, namely: Novi Grad, Prijedor, Oštra Luka, Sanski Most and Ključ. Given that floods were repeated year after year with similar spatial contours, a map with flood risk zones of different types of land use (built areas, forests, arable land and scrub & shrub) was created based on their mapping.

The paper shows the importance of satellite data in the monitoring of climate change and the identification of hazards that arise as a consequence of climate change. CHIRPS satellite precipitation data available from 1981 to near real-time, enabled effective monitoring of changes over a wide time span (1992–2022). The limiting factor of the research was the unavailability of data on precipitation from meteorological stations for the period before 1992 and data on water levels before 2001. The availability of this data would lead to a more accurate identification of time periods with the occurrence of floods in the area. Also, satellite data with a higher spatial resolution than the ones used would contribute to a more precise identification of flooded areas. The results of the research are significant for many

practical issues in the field of safety and flood protection, and the presented data can be useful to competent institutions when developing flood protection strategies and projects, as well as assessing the damage and consequences of floods. A further step forward in relation to the presented research would involve the determination of different scenarios that would include: the types of economic activities in the potentially affected area, industrial facilities that could cause sudden water pollution during floods, and the identification of protected areas at the level research that may be affected by flooding. By integrating these aspects into the existing research, a more accurate and complete "picture" of the consequences that floods can cause in the study area would be obtained.

References

Agency of Statistics of Bosnia and Herzegovina. (2019). *Census of Population, Households and Dwellings in Bosnia and Herzegovina*, 2013.

Amadio, M., Mysiak, J., Carrera, L., & Koks, E. (2016). Improving flood damage assessment models in Italy. *Natural Hazards*, 82, 2075–2088. https://doi.org/10.1007/s11069-016-2286-0

Bai, L., Shi, C., Li, L., Yang, Y., & Wu, J. (2018). Accuracy of CHIRPS satellite-rainfall products over mainland China. *Remote Sensing*, 10(3), 362. https://doi.org/10.3390/rs10030362

Beck, H., Vergopolan, N., Pan, M., Levizzani, V., Van Dijk, A., Weedon, G., Brocca, L., Pappenberger, F., Huffman, G., & Wood, E. F. (2017). Global-scale evaluation of 22 precipitation datasets using gauge observations and hydrological modeling. *Hydrology and Earth System Sciences*, 21(12), 6201–6217. https://doi.org/10.5194/hess-21-6201-2017

Brocca, L., Filippucci, P., Hahn, S., Ciabatta, L., Massari, C., Camici, S., Schüller, L., Bojkov, B., & Wagner, W. (2019). SM2RAIN–ASCAT (2007–2018): Global daily satellite rainfall data from ASCAT soil moisture observations. *Earth System Science Data*, 11(4), 1583–1601. https://doi.org/10.5194/essd-11-1583-2019

Bucchignani, E., Zollo, A. L., Cattaneo, L., Montesarchio, M. & Mercogliano, P. (2016). Extreme weather events over China: Assessment of COSMO-CLM simulations and future scenarios. *International Journal of Climatology*, 37, 1578–1594. https://doi.org/10.1002/joc.4798

Ciric, D., Nieto, R., Ramos, A., Drumond, A., & Gimeno, L. (2018). Contribution of Moisture from Mediterranean Sea to Extreme Precipitation Events over Danube River Basin. *Water*, 10(9), 1182. https://doi.org/10.3390/w10091182

Correia Filho, W. L. F., Oliveira Júnior, J. F., Santiago, D. B., Terassi, P. M. B., Teodoro, P. E., Gois, G., Blanco, C. J. C., Souza, P. H. A., Costa, M., & Santos, P. J. (2019). Rainfall variability in the Brazilian northeast biomes and their interactions with meteorological systems and ENSO via CHELSA product. *Big Earth Data*, 3, 315–337. https://doi.org/10.1080/20964471.2019.1692298

DeVries, B., Huang, C., Armston, J., Huang, W., Jones, J., & Lang, M. (2020). Rapid and robust monitoring of flood events using Sentinel-1 and Landsat data on the Google Earth Engine. *Remote Sensing of Environment*, 240, 11664. https://doi.org/10.1016/j.rse.2020.111664

Dinku, T., Funk, C., Peterson, P., Maidment, R., Tadesse, T., Gadain, H., & Ceccato, P. (2018). Validation of the CHIRPS satellite rainfall estimates over Eastern Africa. *Quarterly Journal of the Royal Meteorological Society*, 144(S1), 292–312. https://doi.org/10.1002/qj.3244

Dong, S., Sun, Y., Li, C., Zhang, X., Min, S. K., & Kim, Y. H. (2021). Attribution of extreme precipitation with updated observations and CMIP6 simulations. *Journal of Climate*, 34, 871–881. https://doi.org/10.1175/JCLI-D-19-1017.1

Funk, C., Peterson, P., Landsfeld, M., Pedereros, D., Verdin, J., Shukla, S., Husak, G., Rowland, J., Harrison, L., Hoell, A., & Michaelsen, J. (2015). The climate hazards infrared precipitation with stations—a new environmental record for monitoring extremes. *Scientific Data*, 2, 150066. https://doi.org/10.1038/sdata.2015.66

Gao, F., Zhang, Y., Chen, Q., Wang, P., Yang, H., Yao, Y., & Cai, W. (2018). Comparison of two long-term and high-resolution satellite precipitation datasets in Xinjiang, China. *Atmospheric Research*, 212, 150–157. https://doi.org/10.1016/j.atmosres.2018.05.016

Gorelick, N., Hancher, M., Dixon, M., Ilyushchenko, S., Thau, D., & Moore, R. (2017). Google Earth Engine: Planetary-scale geospatial analysis for everyone. *Remote Sensing of Environment*, 202, 18–27. https://doi.org/10.1016/j.rse.2017.06.031

Gnjato, S. (2018). Analysis of the Water Discharge at the Sana River. *Гласник/Herald*, 22, 103–116. https://doi.org/10.7251/HER2218103G

IPCC (2021). *Summary for Policymakers, Climate Change 2021: The Physical Science Basis. Contribution of Working Group I to the Sixth Assessment Report of the Intergovernmental Panel on Climate Change*. Cambridge University Press.

Ivanišević, M., Savić, S., Pavić, D., Gnjato, S., & Popov, T. (2022). Spatio-Temporal Patterns of Flooded Areas in the Lower Part of the Sana River Basin (Bosnia and Herzegovina). *Bulletin of the Serbian Geographical Society*, 102(2), 67–82. https://doi.org/10.2298/GSGD2202067I

Katsanos, D., Retalis, A., Tymvios, F., & Michaelides, S. (2016). Analysis of precipitation extremes based on sat-

ellite (CHIRPS) and in situ data set over Cyprus. *Natural Hazards*, 83, 53–63. https://doi.org/10.1007/s11069-016-2335-8

Kidd, C., Becker, A., Huffman, G. J., Muller, C. L., Joe, P., Skofronick-Jackson, G., & Kirschbaum, D. B. (2017). So, how much of the Earth's surface is covered by rain gauges? *Bulletin of the American Meteorological Society*, 98(1), 69–78. https://doi.org/10.1175/BAMS-D-14-00283.1

Kottek, M., Grieser, J., Beck, C., Rudolf, B., & Rubel, F. (2006). World Map of the Köppen-Geiger climate classification updated. *Meteorologische Zeitschrift*, 15(3), 259–263. https://doi.org/10.1127/0941-2948/2006/0130

Kumar, T. V. L., Barbosa, H. A., Thakur, M. K., & Paredes-Trejo, F. (2019). Validation of satellite (TMPA and IMERG) rainfall products with the IMD gridded data sets over monsoon core region of India. In: Rustamov R. B. (Ed.). *Satellite Information Classification and Interpretation*. https://doi.org/10.5772/intechopen.84999

Loew, A., Bell, W., Brocca, L., Bulgin, C. E., Burdanowitz, J., Calbet, X., Donner, R. V., Ghent, D., Gruber, A., Kaminski, T., Kinzel, J., Klepp, C., Lambert, J. C., Schaepman-Strub, G., & Schröder, M. (2017). Validation practices for satellite-based Earth observation data across communities. *Reviews of Geophysics*, 55(3), 779–817. https://doi.org/10.1002/2017RG000562

Maggioni, V., Sapiano, M. R. P., & Adler, R. F. (2016). Estimating uncertainties in high-resolution satellite precipitation products: Systematic or random error? *Journal of Hydrometeorology*, 17(4), 1119–1129. https://doi.org/10.1175/JHM-D-15-0094.1

Meresa, H., Tischbein, B., & Mekonnen, T. (2022). Climate change impact on extreme precipitation and peak flood magnitude and frequency: observations from CMIP6 and hydrological models. *Natural Hazards*, 111, 2649–2679. https://doi.org/10.1007/s11069-021-05152-3

Michaelides, S., Levizzani, V., Anagnostou, E., Bauer, P., Kasparis, T., & Lane, J. E. (2009). Precipitation: Measurement, remote sensing, climatology and modeling. *Atmospheric Research*, 94(4), 512–533. https://doi.org/10.1016/j.atmosres.2009.08.017

Moel, H., Alphen, J., & Aerts, J. (2009). Flood maps in Europe–methods, availability and use. *Natural Hazards and Earth System Science*, 9, 289–301. https://doi.org/10.5194/nhess-9-289-2009

Nghia, B., Pal, I., Chollacoop, N., & Mukhopadhyay, A. (2022). Applying Google earth engine for flood mapping and monitoring in the downstream provinces of Mekong River. *Progress in Disaster Science*, 14, 100235. https://doi.org/10.1016/j.pdisas.2022.100235

Pandey, A., Kaushik, K., & Parida, B. (2022). Google Earth Engine for Large-Scale Flood Mapping Using SAR Data and Impact Assessment on Agriculture and Population of Ganga-Brahmaputra Basin. *Sustainability*, 14(7), 4210. https://doi.org/10.3390/su14074210

Paredes-Trejo, F., Alves Barbosa, H., Venkata Lakshmi Kumar, T., Kumar Thakur, M., & de Oliveira Buriti, C. (2021). Assessment of the CHIRPS-Based Satellite Precipitation Estimates. *IntechOpen*. https://doi.org/10.5772/intechopen.91472

Plank, S. (2014). Rapid Damage Assessment by Means of Multi-Temporal SAR—A Comprehensive Review and Outlook to Sentinel-1. *Remote Sensing*, 6(6), 4870–4906. https://doi.org/10.3390/rs6064870

Popov, T., Gnjato, S., Trbić, G., & Ivanišević, M. (2017). Trends in extreme daily precipitation indices in Bosnia and Herzegovina. *Collection of Papers - Faculty of Geography at the University of Belgrade* , 65(1), 5–24. https://doi.org/10.5937/zrgfub1765005P

Prokić, M., Savić, S., & Pavić, D. (2019). Pluvial flooding in Urban Areas Across the European Continent. *Geographica Pannonica*, 23(4), 216–232. https://doi.org/10.5937/gp23-23508

Raghavan S. (2013). *Radar Meteorology*. Springer Dordrecht. https://doi.org/10.1007/978-94-017-0201-0

Republika Srpska Institute of Statistics. (2017). *Census of population, households and dwellings in Republika Srpska*, 2013.

Rincón-Avalos, P., Khouakhi, A., Mendoza-Cano, O., López-De la Cruz, J., & Paredes-Bonilla, K. M. (2022). Evaluation of satellite precipitation products over Mexico using Google Earth Engine. *Journal of Hydroinformatics*, 24(4), 711–729. https://doi.org/10.2166/hydro.2022.122

Sabljić, L., & Bajić, D. (2021). Mapping of flooded areas using remote sensing on the example of the Sana river. *Гласник/Herald*, 25, 109–120. https://doi.org/10.7251/HER2125109S

Sarkadi, N., Pirkhoffer, E., Lóczy, D., Balatonyi, L. B., Geresdi, I., Fábián, S. Á., Varga, G., Balogh, R., Gradwohl Valkay, A., Halmai, Á., & Czigány, S. (2022). Generation of a flood susceptibility map of evenly weighted conditioning factors for Hungary. *Geographica Pannonica*, 26(3), 200-214. https://doi.org/10.5937/gp26-38969

Samuele, P., Filippo, S., & Enrico, B-M. (2021). Multi-temporal mapping of flood damage to crops using sentinel-1 imagery: a case study of the Sesia River (October 2020). *Remote Sensing Letters*, 12(5), 459–469. https://doi.org/10.1080/2150704X.2021.1890262

Tabari, H. (2020). Climate change impact on flood and extreme precipitation increases with water availability. *Scientific Reports*, 10, 13768. https://doi.org/10.1038/s41598-020-70816-2

Tran, K. H., Menenti, M., & Jia, L. (2022). Surface Water Mapping and Flood Monitoring in the Mekong Delta Using Sentinel-1 SAR Time Series and Otsu Threshold. *Remote Sensing*, 14(22), 5721. https://doi.org/10.3390/rs14225721

Vanama, V., Mandal, D., & Rao, Y. (2020). GEE4FLOOD: rapid mapping of flood areas using temporal Sentinel-1 SAR images with Google Earth Engine cloud platform. *Journal of Applied Remote Sensing*, 14(3), 034505. https://doi.org/10.1117/1.JRS.14.034505

Ward, P. J., Jongman, B., Weiland, F., Bouwman, A., van Beek, R., Bierkens, M., Ligtvoet, W., & Winsemius, H. (2013). Assessing flood risk at the global scale: Model setup, results, and sensitivity. *Environmental Research Letters*, 8, 044019. https://doi.org/10.1088/1748-9326/8/4/044019

Wu, W., Li, Y., Luo, X., Zhang, Y., Ji, X., & Li, X. (2019). Performance evaluation of the CHIRPS precipitation dataset and its utility in drought monitoring over Yunnan Province, China. *Geomatics, Natural Hazards and Risk*, 10(1), 2145–2162. https://doi.org/10.1080/19475705.2019.1683082

Zhang, Y., Wu, C., Yeh, P. J., Li, J., Hu, B., Feng, P., & Jun, C. (2022). Evaluation and comparison of precipitation estimates and hydrologic utility of CHIRPS, TRMM 3B42 V7 and PERSIANN-CDR products in various climate regimes. *Atmospheric Research*, 265, 105881. https://doi.org/10.1016/j.atmosres.2021.105881